

CURRENT AND POTENTIAL APPLICATIONS OF INDUCTIVELY COUPLED PLASMA (ICP)-
ATOMIC EMISSION SPECTROSCOPY (AES) IN THE EXPLORATION, MINING, AND
PROCESSING OF MATERIALS

Velmer A. Fassel

Ames Laboratory-ERDA and Department of Chemistry, Iowa State University
Ames, Iowa 50011, USA

Abstract - The first papers describing the potential advantages of using inductively coupled plasmas as vaporization-atomization-excitation sources for the atomic emission determination of the elements appeared in the literature approximately ten years ago. During the elapsed decade, continuing studies in a relatively small number of laboratories have led to striking advances in the scope of application of this analytical concept. With state of the art systems, it is now possible to determine all of the metals, metalloids, noble gases, and hydrogen at the major, minor, trace, and ultratrace level in a viable practical manner. In principle, all of these elements can be detected and determined simultaneously or sequentially under a single set of operating conditions. In this review the formation and the properties of these plasmas will be summarized and the present capabilities of ICP-AES with reference to such figures of merit as powers of detection, simultaneous multielement capability, applicability to the analysis of microliter or microgram samples, interelement effects, applicability to the direct excitation of liquids, solids, and gases, cost, accuracy, precision and dynamic range will be reviewed.

INTRODUCTION

The production of materials, beginning with the search for and the assessment of sources of supply and continuing through the beneficiation, processing, and manufacture stages, poses many analytical problems. To meet the many elemental characterization and quantitation needs, it is desirable to have a single analytical facility that satisfies the following analytical requirements:

1. Applicable to all elements.
2. Simultaneous multielement determination capability at the major, minor, trace and ultratrace concentration level.
3. No interelement interference effects.
4. Applicable to the analysis of microliter or microgram sized samples.
5. Applicable to the analysis of solids, liquids, and gases with minimal preliminary sample preparation or manipulation.
6. Capable of providing rapid analyses; amenable to process control.
7. Acceptable facility requirements and cost/analysis.
8. Acceptable precision and accuracy.
9. Non destructive.
10. Portable.

The above list essentially defines the performance characteristics of an ideal simultaneous multielement analytical facility. Indeed, one of the major challenges in the fields of analytical chemistry and spectroscopy has been the development of the basic science, the investigative methods, and the hardware components of just such a system. If achieved, a single facility would then replace, or substitute for, a multitude of traditional chemical or instrumental schemes for elemental analyses.

Because there is no known analytical technique or system that fulfils completely the criteria listed above, it is important to assess, as perceptively as we can, whether new approaches may meet these requirements to a higher degree than present technologies. One of the most promising candidates is based on utilizing the classical approach to simultaneous analysis, namely, atomic emission spectroscopy. Rather than utilizing conventional arc, spark, or transferred plasmas as sample vaporization-atomization-excitation and ionization sources, a new type of analytical plasma is employed. This is an electrodeless argon plasma formed at atmospheric pressure, and sustained by inductive coupling to high frequency magnetic fields. This plasma possesses unique physical properties that make it a remarkable vaporization-atomization-excitation-ionization source for elemental analytes, at the major, minor trace and ultratrace level, by atomic emission techniques.

MULTIELEMENT ANALYSIS, BY ATOMIC EMISSION SPECTROSCOPY (AES)

The observation of free atoms or ions in emission has been the classical approach to simultaneous multielement determinations. In contrast to conventional atomic absorption or atomic fluorescence spectroscopy techniques, there is no requirement for an auxiliary primary source for each element to be determined. It is only necessary to devise an acceptable scheme for generating free atoms of the analyte and for exciting their emission spectra. The appropriate analyte emission lines may then be isolated and their intensities measured in the classical way, by employing multichannel polychromators of the type shown in highly schematic form in Fig. 1.

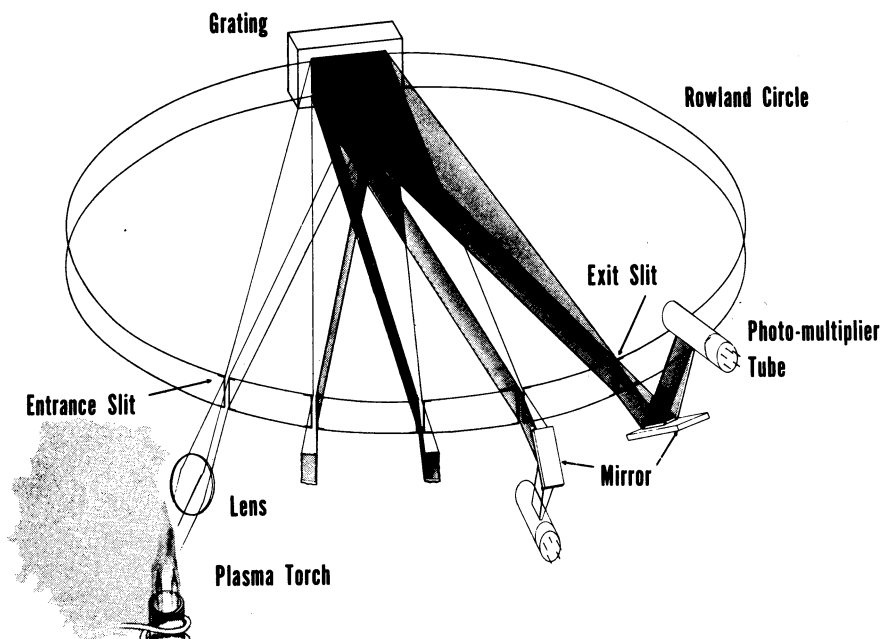


Fig. 1. Schematic diagram of a typical atomic emission polychromator.
(Reproduced from (8) by permission of Anal. Chem.)

In the minds of many analysts the importance of AES as an analytical tool for the determination of trace elements has declined during the past decade for several reasons. The foremost of these reasons rests in the remarkable success flame AAS has achieved in the years since Walsh published his first paper on the application of atomic absorption spectroscopy (AAS) to chemical analyses (1). In view of this success, it is not human nature to turn to alternate techniques to perform the same tasks. In recent years, AES also has fallen into some disrepute, not because of valid scientific or technological reasons, but because of less than rigorous claims made in the AAS literature. These claims were related to the alleged superiority of observing free atoms in absorption rather than in emission with reference to such figures of merit as detection limits and freedom from interelement effects. Many of these claims have not withstood the test of time, but they were repeated often enough to generate negative reactions to the use of atomic emission for trace analysis purposes.

Another factor that may have contributed to the decline of AES as a trace element technique has been the occasional assertion (they are still being made) that multichannel spectrometers of the type shown in Fig. 1 are too complex, too cumbersome, too difficult to keep in alignment and too expensive. I have the impression that the authors of these assertions may not be aware of the technological improvements in these spectrometers over the past thirty years. It is a revealing experience to visit a modern steel or aluminum control laboratory and observe that these instruments are employed for the determination of up to ten or more major and minor constituents, at rates of up to 600 analyses/hour (on 40 to 50 samples), often under alarming environmental conditions, with relative standard deviations of 0.5 to 1 for twenty-four hours per day. The total number of major, minor, and trace constituents determined in this way by the instruments in current use must be orders of magnitude more than by all other trace element determinations made by atomic absorption methods.

In recent years the potential importance of AES for elemental analysis has made a sharp upward turn, primarily because of major developments in the heart of any AES analytical system, i.e., the vaporization-atomization-excitation source. These advances have resulted primarily

from the recognition that state of the art sources possessed properties that were far less than ideal.

Inductively coupled plasmas

The pioneering studies on inductively coupled plasmas by Reed (2) in the early 1960's and his development of ingenious techniques for stabilizing these plasmas set the stage for a number of subsequent interesting applications (4). Although Reed recognized that these plasmas offered attractive possibilities for vaporizing, atomizing and exciting the spectra of material injected into them (3), the initial analytical studies apparently were undertaken independently in two widely separated laboratories, one at Albright and Wilson in Oldbury, England (5) and the other at the Ames Laboratory, Iowa State University (6). Later, a succession of workers in various countries also explored their potential. The analytical applications of these plasmas have been reviewed recently by Fassel and Kniseley (7,8) and by Greenfield and associates (9).

The general goals of our early studies, and undoubtedly those of others as well, were essentially threefold: (a) to ascertain whether these plasmas could in fact be operated under the low power conditions that would be comfortable to analytical chemists; (b) to study the behavior of the plasmas upon the injection of samples as solutions; and (c) to evaluate the analytical performance. A specific goal of these early studies was to ascertain the potential of these plasmas for trace multielement determinations. For these applications, detection limits or powers of detection are primary figures of merit. If detection limits are measured on a signal/noise bases, the numbers measured reflect accurately the analyte and background signal levels and their stabilities and provide the analyst a sound numerical basis for comparing capabilities. The experimental values reported by Greenfield et al. (5) and Wendt and Fassel (8) in the early 1960's did not provide encouragement; the detection limits were inferior to those reported in the literature for atomic absorption spectroscopy. The striking improvements in the ICP-AES values during the past twelve years is shown by the data summarized in Table I.

TABLE 1. Inductively coupled plasma detection limits ($\mu\text{g/ml}$)

	1964	1965	1965	1969	1971-72	1975-76
	Greenfield et al. (5)	Wendt Fassel (6)	Greenfield et al. (10)	Dickinson Fassel (11)	Fassel (12)	Boumans-de Boer (13) Olson-Haas-Fassel (14)
Al	50	3	0.5	0.002	0.002	0.0004 (14)
As	--	25	--	0.1	0.04	0.002 (14)
Ca	1	0.2	0.005	--	0.00007	0.000001 (13)
Cd	--	20	--	0.03	0.002	0.00007 (14)
Co	--	--	0.2	0.003	0.003	0.0001 (14)
Cr	20	0.3	--	0.001	0.001	0.00008 (14)
Cu	10	0.2	0.01	--	0.001	0.00004 (14)
Fe	--	3	0.05	0.005	0.005	0.00009 (13)
La	--	50	--	0.003	0.003	0.0001 (13)
Mg	5	2	0.03	--	0.0007	0.000003 (13)
Mn	10	1	0.05	--	0.0007	0.00001 (14)
Ni	5	1	--	0.006	0.006	0.0002 (13)
P	--	10	0.8	0.1	0.04	0.015 (13)
Pb	--	--	--	0.008	0.008	0.001 (14)
Si	--	3	--	--	0.01	--
Sn	--	50	4	--	0.3	0.003 (13)
Sr	--	.09	--	0.00002	0.00002	0.000003 (13)
Ta	--	16	--	0.07	--	--
Th	--	40	--	0.003	--	--
V	--	--	0.1	0.006	--	0.00006 (13)
W	--	3	--	0.002	--	0.0008 (13)
Zn	--	30	4	0.009	0.002	0.0001 (14)
Zr	--	15	--	0.005	--	0.06 (13)

These improvements resulted primarily from progressive refinements in the following: (a) reduction of radiofrequency interference with the recording electronics; (b) more effective impedance matching between the high frequency generator and the plasma and greater control of forward power regulation; and (c) improvements in techniques for generating aerosols of analyte solutions and in their injection into properly shaped plasmas.

The powers of detection summarized in the last column of Table 1 reflect a magnitude and uniformity difficult or impossible to achieve by any other analytical technique. The realization that these powers of detection can be achieved under exactly the same experimental conditions employed for the determination of major constituents suggests that these plasmas possess distinctive properties not found in other atomization-vaporization-excitation

sources. It is therefore appropriate to review the operating principles and properties of these plasmas before discussing their analytical applications.

Although a variety of plasma torch configurations and magnitude and patterns of gas flow have been described, the combinations recommended by Fassel and associates (7,8,15) are more commonly used, especially in the commercial instruments now available. In the discussion that follows, specific reference is made to the configuration used in our laboratories, although the scientific principles and operating procedures apply to other as well. As shown in Fig. 2, the plasma is formed and sustained at the open end of an assembly of quartz tubes. The open end of the outermost tube is surrounded by the induction coil, which is connected to a high frequency current generator. In our systems the latter provides forward powers of up to ≈ 3 kW at a frequency of 27.12 MHz. To form a stable plasma, a pattern of two, or sometimes three, argon flows, as shown in Fig. 2, is used. The auxiliary gas flow facilitates initiation of the plasma and prevents overheating of the intermediate tube during initiation. The auxiliary flow is not normally used when aqueous aerosols are introduced into the plasma. When oil samples are nebulized, the auxiliary flow prevents the formation of carbonaceous deposits on the intermediate tube. When the various flows are adjusted properly, the plasma is readily initiated by "tickling" the quartz tube inside the coil with a Tesla discharge. The plasma is then formed spontaneously after a few popping flashes.

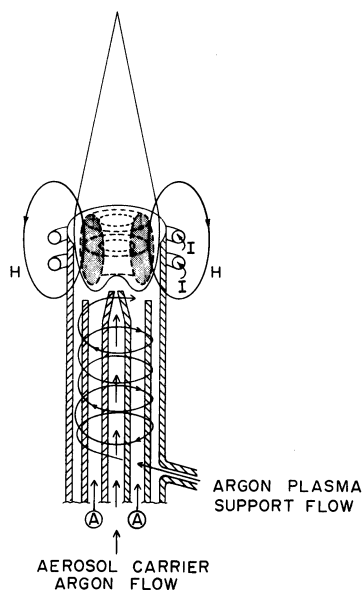


Fig. 2 Typical inductively coupled plasma configuration. Flow A is optional, as explained in text.

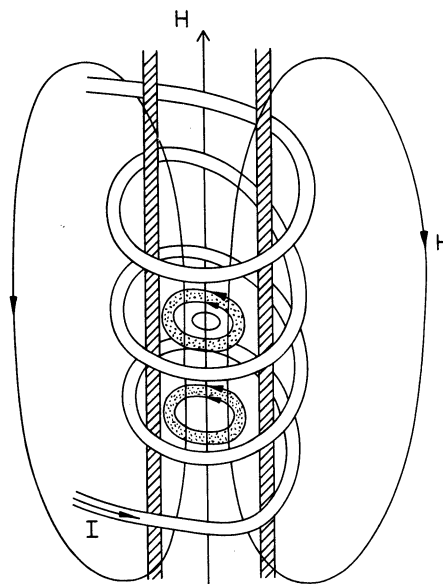


Fig. 3 Magnetic fields (H) and eddy currents (shaded) generated by high frequency currents (I) flowing through coil. (Reproduced from (8) by permission of Anal. Chem.)

To appreciate the course of events that lead to the formation of the plasma, it should be recalled that the high-frequency currents flowing in the induction coil generate oscillating magnetic fields whose lines of force are axially oriented inside the quartz tube and which follow elliptical closed paths outside the coil as shown schematically in Fig 3. The induced axial magnetic fields, in turn, induce the seed of electrons and ions produced by the Tesla coil to flow in closed annular paths inside the quartz tube space. This electron flow - the eddy current - is analogous to the current flow in a short-circuited secondary of a transformer. Because the induced magnetic fields are time-varying in their direction and strength, the electrons are accelerated on each half cycle. The accelerated electrons (and ions) meet resistance to their flow, Joule or ohmic heating is a natural consequence, and additional ionization occurs. The steps just discussed lead to the almost instantaneous formation of a plasma of extended dimensions whose unique properties and characteristics make it a very promising excitation source.

Thermal isolation of plasma

The plasma formed in this way attains gas temperatures in the 9000-10,000°K range (16) in the region of maximum eddy current flow schematically indicated by the cross hatching in Fig. 2. At these temperatures it is necessary to provide some thermal isolation of the plasma to prevent overheating of the quartz containment cylinder. This isolation is achieved by Reed's vortex stabilization technique (2,3) which utilizes a flow of argon that is introduced tangentially in the manner shown in Fig. 2. The tangential flow of argon, which is typically in the 10 to 15 liters/min range for the apparatus shown, streams upward, cooling the inside

walls of the outermost quartz tube and centering the plasma radially in the tube. The tangential flow of argon also serves as the primary sustaining flow. The plasma itself is anchored near the exit end of the concentric tube arrangement.

In addition to the vortex stabilization flow, there is another Ar flow of approximately 1 to 1.5 liters/min that transports the sample to the plasma either as an aerosol, a powder, or a thermally generated vapor. The total argon flow required is therefore in the 11 to 17 liters/min range. Thus, the operating cost of these plasmas, exclusive of electrical power, is lower than the cost of the gases needed to operate the nitrous oxide-acetylene flame commonly used in AAS.

Preliminary sample preparation

The most commonly used approach for introducing sample material into the plasma is based on the injection into the plasma of aerosols generated from aqueous or organic solutions of the sample either by pneumatic or by ultrasonic nebulization techniques; typical systems are illustrated in Figs. 4 and 5. The analysis of samples in this form is obviously most convenient for the direct analysis of liquids of various types, including process streams, edible oils, liquid fuels, and body fluids. Aerosols of solid metallic particles produced by ultrasonic nebulization of molten metals have also been introduced into the plasma (18).

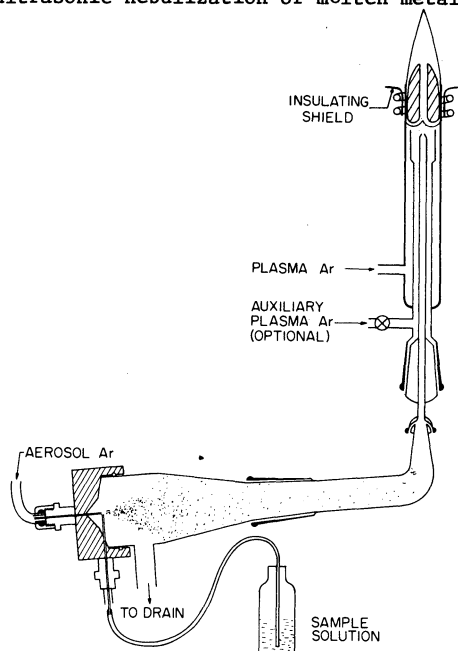


Fig. 4. Typical pneumatic nebulization facility. The crossed-needle type nebulizer is described in reference (19).

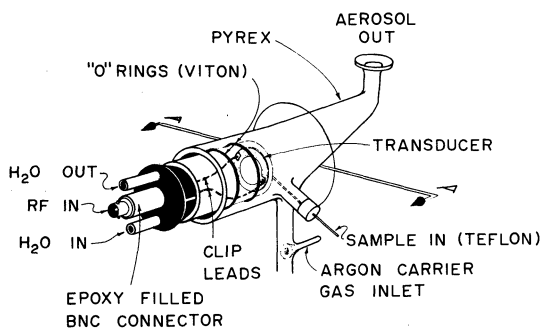


Fig. 5. An ultrasonic nebulization facility. This nebulizer is described in reference (14).

Solid samples may be dissolved by a variety of conventional aqueous or fusion dissolution methods, but these procedures are subject to several limitations. First, one of the major goals in the metals industry is the formulation of alloys with increasing corrosion stability. The greater the success in this endeavor, the less successful the chemist in dissolving the sample. Second, the reagents used for the dissolution as well as the containers are always potential sources of contamination. Third, dissolution causes considerable dilution of the sample and is therefore responsible for a loss of power of detection, particularly for trace constituents. For example, sample solutions are normally used at total metal ion concentrations of 0.1-0.5%. These concentrations represent a dilution factor of from 1000 to 200, respectively. Fourth, dissolution of the sample is often the most time consuming step in the analytical cycle.

The direct sampling of solids, without prior dissolution, would be clearly advantageous. The transformation of solid metal samples into aerosols that are subsequently injected into the plasma has been achieved in several ways. In one device, now commercially available in a hand-held version (20,21), the cold cathode termination of a dc arc in argon is utilized to generate the aerosol. The cathode spot (or spots) of the arc discharge moves rapidly over the surface of the sample, the sampling area being defined by a boron nitride insulator against which the sample is sealed (see Fig. 6). The removal of material from the sample surface appears to be related to high frequency (0.3 to 1 MHz) oscillations in the voltage drop across the arc that approach the open circuit value. These pulses evidently correspond to the formation of randomly sampled pits. There is little or no indication of preferred erosion of inclusions or grain boundaries. The ejected particulates,

which have typical diameters in the micron region, are transported to the plasma by the same carrier gas argon flow that ejects sample material into the axial channel of the discharge. The aerosol is readily transported through flexible tubing over distances of up to 10 to 20 meters thus allowing remote sampling.

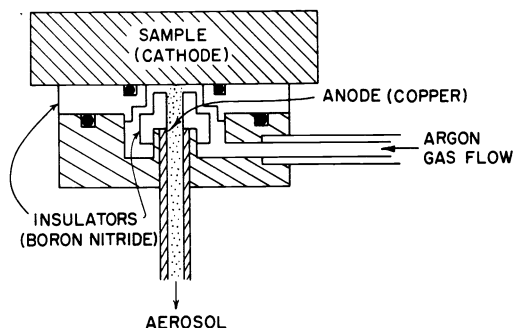


Fig. 6. Device for the direct generation of aerosols from solid metal samples.

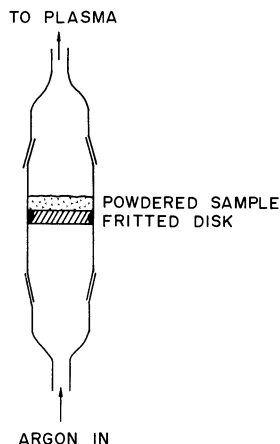


Fig. 7. Device for introducing finely powdered samples into the plasma.

Powdered samples may be injected directly into the plasma. In fact, one of Reed's initial applications of these plasmas was directed toward utilizing the plasma as a high temperature source for melting powders as a first step in growing refractory single crystals (2,3) in the tail flame. The observation by Reed that the finer particles of refractory powders were completely vaporized thus presaged subsequent efforts to evaluate the potential analytical utility of injecting powdered samples directly into the plasma

Fluidized bed chambers have been used by several investigators to effect the continuous injection of finely divided powders into the plasma. The powder, which should have a particle size distributions that peaks in the 1 to 3 μm range, may be transformed into a dust either by vibration of an appropriate sample container (22,23) or by the passage of the aerosol carrier argon flow through a coarse porosity glass disk on which the powder is supported (7,23,24). A simple device for performing the latter operation is shown in Fig. 7. Mechanical vibration of this or similar devices assists in the formation of a fluidized bed. The same argon flow normally employed in injecting liquid aerosols into the plasma continuously transports some of the suspended dust cloud to the plasma. Although the powders experience the gas temperatures shown in Fig. 8 in their transit through the plasma, (see discussion below), it should be recognized that the transfer of thermal energy from the gas phase to solid particles is rather inefficient. Recognition should also be given to the fact that dehydrated aerosol droplet residues range in size from 0.01 to 0.1 μm , whereas it is not practical to comminute solid samples beyond the 1 μm range. Thus atomization efficiencies as a general rule would be expected to be less for solid powdered samples. Because the powders may not be completely atomized, the freedom of interelement effects achieved when liquid aerosols are injected into the plasma may be prejudiced. For example, Hoare and Mosteyn's observations (22) that the preparative history of samples and reference standards should be as nearly identical as possible is supportive of this expectation.

Although the fluidized bed technique has been used successfully for the analysis of several types of powdered samples, particle size and density discrimination effects and aggregation of fine particles may limit the scope of application of this approach. Greenfield et al. have correctly assessed the present status of direct powder analysis when they stated "a general, practical solution to the several problems of injecting powders into plasmas and performing quantitative analysis has yet to be found" (9).

Sample injection into plasmas

If plasmas are to be effective atomization and excitation sources, the sample aerosols should be injected efficiently into the plasma and remain in the interior high-temperature environment as long as possible. These physical conditions have been difficult or impossible to attain in non-ICP plasma systems suggested for analytical purposes (7). The ICP poses problems as well. In the ICP the gases are heated internally, causing thermal expansion in a direction perpendicular to the exterior surface of the plasma. There is also an excess magnetic pressure along the axial channel of the plasma (25). According to Chase (25) the magnetic pressure drops toward the axial channel of the plasma, causing a

small inward radial flow of the plasma. This inward flow may be viewed as generating both a beneficial and a deleterious effect. The inward radial flow of plasma should assist in the confinement of the analyte streams in the midsection of the plasma core, once the sample aerosol is injected into the plasma. The electron and ion drift toward the center transmit their motion by momentum exchange to the neutral particles (4). This magnetic pumping effect, however, builds up the kinetic pressure along the axial channel of the plasma, causing an axial flow of plasma toward the floor and tail flame of the plasma. The consequence of the thermal expansion and magnetohydrodynamic thrusts is that sample material tends to by-pass the plasma. The sample injection process must therefore overcome these thrusts, without causing collapse of the plasma.

The skin depth effect of induction heating has been used to good advantage in providing a partial solution to this problem. When the high frequency current flow in the coil is increased from say 4 to 30 MHz, the region of the highest eddy current density moves toward the outer surface of the plasma. At frequencies of ≈ 25 to 30 MHz, an incipient annular or "doughnut" plasma shape is developed. Because the hole possesses a somewhat lower temperature than the "doughnut", it offers less resistance to the injection of sample material. The annular shape can be further developed by optimizing the flow velocity and pattern of the carrier gas that injects the sample into the plasma. Thus, the degree to which the annular or toroidal shape is developed can be controlled by the frequency of the primary current generator, the flow velocity of the carrier gas stream, and the aerodynamics of the carrier gas flow stream (11,26). At ≈ 30 MHz, a carrier gas flow of ~ 1 l/min assures effective injection of sample into the plasma, if properly designed injection orifices are used (7,11,15). When the plasma is viewed from the bottom or the top under these conditions, it has the appearance of a doughnut.

Properties of the plasma

The plasma discussed above possesses unique physical properties that make it a remarkably successful vaporization-atomization-excitation source. These properties can be interpreted by referring to the scale drawing of the plasma in Fig. 8. According to our temperature measurements above the coil, and by extrapolative estimation down into the induction region (16), the sample particles experience a gas temperature of ≈ 7000 - 8000 K as they pass through the eddy current tunnel. By the time the sample decomposition products reach the observation height of 15 to 20 mm above the coil, they have had a residence time of ≈ 2 msec at temperatures ranging downward from ≈ 8000 (estimate) to ≈ 5500 K. Both the residence times and the temperatures experienced by the sample are approximately twice as great as those found in $N_2O-C_2H_2$ flames - the hottest flame commonly used in analytical spectroscopy. The combination of high temperatures and relatively long sample-plasma interaction times should lead to complete sample vaporization and a high, essentially total, degree of atomization of the analyte species. Once the free atoms or ions are formed, they occur in a chemically inert environment, as opposed to the violently reactive surroundings in combustion flames. Thus, their lifetime, on the average, should be longer than in flames.

With reference to interelement or matrix interferences in the vaporization-atomization-excitation process, it is important to emphasize that the sample or its decomposition products are heated indirectly via convection, conduction and radiation as they pass through the eddy current "tunnel". The inward radial flow of plasma produced by the "magnetic pumping" effect may in addition provide electrical screening of the analyte vapor cloud from the load coil. As a consequence, there appears to be only a negligible interaction of the sample with the sustaining eddy current flow. For reasons not yet understood, the addition of easily ionizable elements to the plasma causes remarkably low ionization type interferences on analytes of low ionization energies, in contrast to the large effects commonly observed in flames.

The plasma possesses other unique advantages. First, after the free atoms are formed, they flow downstream in a narrow cylindrical radiating channel. The optical aperture or viewing field of conventional spectrometers can be readily filled by this narrow radiating channel. In this way, the radiation emitted by the free atoms or ions is used effectively. Second, at the normal height of observation, the central axial channel containing the relatively high number density of analyte free atoms or ions has a rather uniform temperature profile (16). The number density of free atoms in the hot argon sheath surrounding the axial channel is far lower. Under these conditions, the analyte free atoms or ions tend to behave as an optically thin emitting source. If a large range of emission intensities can be accommodated linearly by the measurement system, linear analytical calibration curves covering five orders of magnitude change in concentration can be readily achieved. Thus, the variable dilutions often needed in flame AAS techniques are essentially eliminated.

Several unique advantages also accrue from the simple fact that the optimum region of analyte emission is separated spatially from the high spectral background region in which free atom formation occurs. Thus, sample vaporization and atomization occur in the high-temperature environment of the core of the plasma, which otherwise has little analytical utility because of the intense continuum emission. The analyte free atoms or ions released in the core may then be observed downstream in temperature environments ranging downward from $6500^\circ K$ to typical combustion flame temperatures.

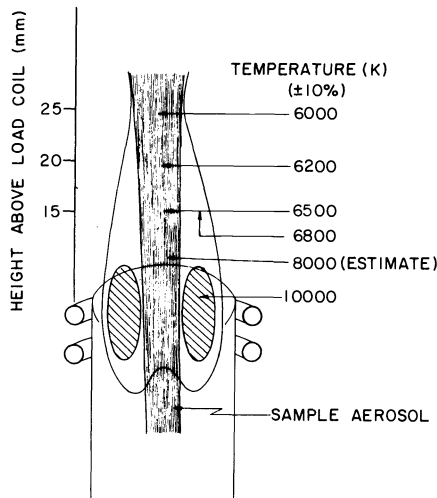


Fig. 8. Temperatures in the plasma as measured by the spectroscopic slope method (16).

Other advantages of these plasmas are worthy of note. No electrodes are used. Therefore, contamination from the electrodes normally used in other plasmas is eliminated. Because the plasma operates on nonexplosive gases, the system can be used in locations where combustibles are not allowed.

Description of spectra emitted. The plasma has the overall appearance of a very intense, brilliant white, nontransparent core and a flame-like tail. The plasma core, which resides inside and extends a few millimeters above the induction coil region, emits an intense continuum in addition to a rather fully developed spectrum of neutral argon. The continuum presumably arises from ion recombination processes and bremsstrahlen emission. As noted above, radiation from the plasma core has little analytical utility. The core fades into a second recognizable zone of the plasma which extends from approximately 1 to 3 cm above the induction coil. This zone is also bright but slightly transparent. In the mid-to-upper regions of this zone, the continuum emission is sharply reduced by several orders of magnitude from the core emission. Structural background consists of Ar lines, the OH band emission between 260-325 nm, and weak band emission from NO, NH, CN and C₂. The tail flame or third zone of the plasma is barely visible when distilled water is nebulized but assumes typical flame colors when analytes are added to the plasma. The axial passage of the sample aerosol and its decomposition products through the plasma is clearly visible.

The fact that many of the sensitive lines of the elements originated from singly ionized species was recorded by Dickinson and Fassel (11) in 1969 and later by Souillart and Robin (27). Still later when Boumans and de Boer rediscovered this fact (13), they expressed surprise at their observations. The latter workers have provided a useful comparison of powers of detection of selected neutral atom and ion lines of thirteen elements. Wavelength tables of the most sensitive lines observed in the plasma may be found in several publications (9,11,13,27).

Compromise experimental variables. The analytical performance of these plasmas may be greatly affected by the choice of experimental parameters. If the assumption is made that the choice of frequency of the current flowing in the coil, the torch configuration, and the pattern of gas flows assures effective injection of the sample into the axial channel of the plasma, the remaining dominant experimental parameters are: (a) power input into the plasma; (b) Ar carrier-gas flow-rate; (c) observation height. Although the nominal power of the generators employed for analytical purposes has ranged from 2 to 15 KW, most investigators have worked in the 2 to 5 KW range (9) and this trend has been reflected in the commercial units. Most of the advantages cited by Greenfield et al. (9) for using higher power cannot be disputed, but documentation that greater "sensitivity", more frequent improvement in precision, and more effective elimination of chemical interferences is achieved appears to be lacking. The primary disadvantages of working at the higher power are the increased size and cost of the generator and the higher consumption of electricity and support and coolant gases. It has been estimated that ≈ 50 to 70% of the nominal power is actually transferred to the plasma (2,9,26). Thus, for most of the analytical studies reported to date at the lower power level, the actual power dissipated in the plasma is believed to be in the 0.5 to 1 KW range.

In considering the role played by the other two dominant experimental variables - aerosol carrier Ar flow rate and observation height - it is instructive to refer to several of the

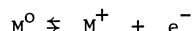
early papers published on the analytical applications of these plasmas (5,7,11,17). These early reports established a pattern of observations which indicated that a remarkably low degree of interelement interference effects were observed under the same experimental conditions employed for determining the detection limits. This was true whether the analyte free atoms released in the plasma were observed in emission or absorption. In two of these papers (11,17), observation heights giving maximal powers of detection for individual elements were tabulated. These observations were later confirmed by Boumans and de Boer (28), who also showed that carrier gas flow affected the powers of detection observed. Boumans and de Boer concluded that for simultaneous multielement analysis at high detection power, two pairs of values of observation height and carrier gas flow would provide optimal parameters for most elements in the periodic system (28). Because of the excellent powers of detection observed in our laboratory at fixed observation heights and gas flows, and the general experience that improvement factors greater than five could be rarely achieved by optimizing these parameters, the concept of a single "compromise" set of experimental parameters (forward power, observation height, and carrier gas flow) for the detection and determination of all metals and metalloids was strongly supported (8,15). Further supporting evidence that compromise parameters can be identified has been provided by Boumans and de Boer (13).

Interelement Interferences

The ultimate scope of application of any analytical technique is determined by many operational and performance factors. One of the most important of these is the degree of freedom from interelement interactions or interferences ("matrix effects") exhibited by the analytical method. These interferences by concomitants (constituents in the sample other than the analyte) may be spectral or non-spectral in nature. The former arise from incomplete isolation of the radiation emitted by the analyte from other radiation detected by the instrument. These interferences are discussed in more detail in the following section.

For interelement interferences other than spectral, the analyte signal itself is directly affected. In my discussion above on the properties of these plasmas, I have noted the physical aspects that lead to expectations that interelement interactions in the plasma would be far less than in other vaporization - atomization - excitation sources. These expectations have been repeatedly confirmed. One of the classical analyte vaporization - dissociation - atomization interferences is the suppression of Ca free-atom formation in the presence of increasing concentrations of Al. This suppression has been attributed to the formation of refractory compounds and to the occlusion of the Ca analyte in a refractory oxide matrix (30,31). In flames and many arc discharges, the Ca emission is observed to decrease toward zero with increasing Al concentrations. The behavior in the ICP is shown in the bottom portion of Fig. 9. The absence of any depression at low Al/Ca molar ratios verifies that no measurable analyte vaporization - dissociation - atomization interference occurs. There is a gentle decrease in intensity up to molar ratios of 100(0.1350 ug Al/ml); for the neutral atom line this depression is remarkably low (~2%). Thus, if analytical calibration curves established for the determination of Ca in "pure" water were applied directly to the determination of Ca in Al, an error of only ~2% of the amount present would be experienced, if the Al sample concentration in solution was selected to be 0.14 wt %

The ionization interferences commonly observed in flames, arc, and spark discharges are a manifestation of the shift in the ionization equilibrium of the analyte (M):



The introduction of easily ionizable elements, such as the alkalis, into the plasma would be expected to increase the electron number density in the axial channel of the plasma to such a level that the equilibrium is shifted to the left, causing an enrichment of neutral atom lines and a depression of ion lines of the analyte. The top portion of Figure 8 shows that even for the analyte Ca, which has a relatively low ionization potential (6.11 eV), the ionization interference effect is surprisingly small. Thus, at a Na concentration of 0.2 wt %, the analytical equivalent of determining Ca in NaCl, simple aqueous reference standards would introduce only a 5 to 10% bias.

It is quite certain that factors other than ionization effects play a role in the trends of the curves plotted in Fig. 9. For example, the increasing concentrations of Na may have been great enough to produce a transport interference caused by changes in the physical properties of the solution and their effect on the aerosol generation process. A definitive interpretation of the magnitude and trends of the small but significant interelement effect observed at the higher concentration levels of the concomitants requires a far more detailed knowledge than is now available of the spatial distribution of analyte free atoms and temperature, of the ionization equilibria prevailing, and of the role played by the Ar sustaining gas. Our inability to interpret these results in a more definitive manner should not detract from the significance of the results, namely, that interelement interactions are small or insignificant for reasonable changes in the concentration of concomitants under the same experimental conditions selected for obtaining excellent powers of detection.

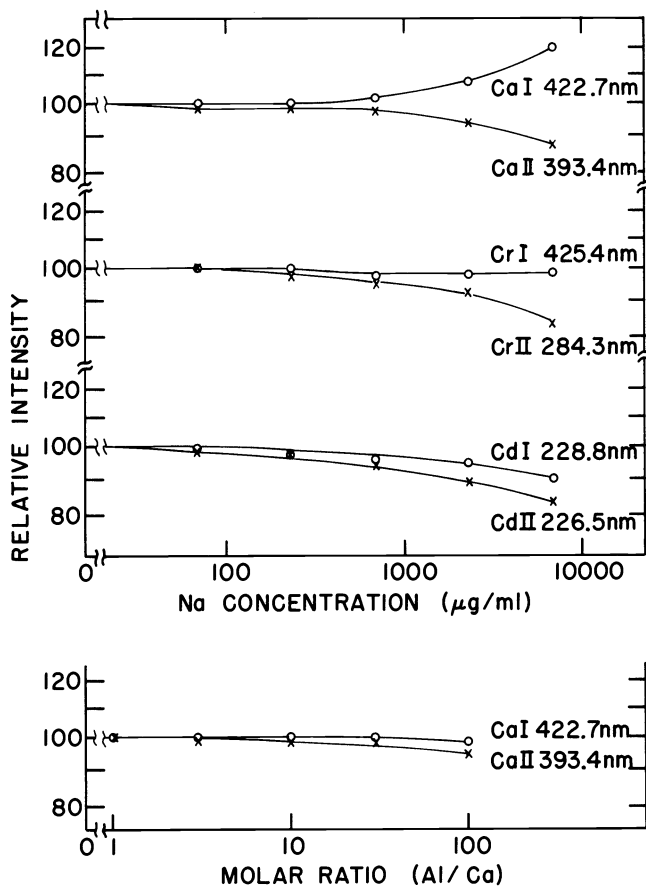


Fig. 9. (Top) Effect of increasing concentrations of Na on Ca, Cr, and Cd neutral atom and ion emission intensities. (Bottom) Effect of increasing concentrations of Al on Ca emission intensities.

One of the practical implications of these observations is the interesting and potentially very valuable possibility of establishing single analytical calibration curves for the determination of an analyte in a variety of matrices. Documentary evidence that the plasma offers this promise is found in Table 2.

TABLE 2. Effect of Concomitants on the Emission of Molybdenum Lines

Concomitant (2500 µg/ml)	Relative Intensity	
	Mo I 390.3 nm	Mo II 281.6 nm
None (distilled H ₂ O)	100	100
K	102	97
Na	105	94
Al	103†	95†
Cu	100	100
Zn	101	100

† Corrected for spectral interference by concomitant

These data show that a complete change of the matrix in solution induced a maximum change in signal of only - 6% (for the Na matrix). In contrast, in a high temperature N₂O - C₂H₂ flame atomization cell, the matrix effects ranged up to a factor of three (32). In another study worthy of note, Butler et al. (33) demonstrated that Al, Cr, Cu, Mn, and Ni could be determined accurately in low and high alloy steels in solution by relating the analyte line intensities to analytical calibration curves that were based on reference

solutions containing only Fe and the analyte. No attempt was made to match the overall composition of the steel samples and the synthetic reference solutions employed for calibration purposes. The accuracy of the analysis was assessed by analyzing a series of National Bureau of Standards (NBS) Reference Samples. Three different ICP systems with different characteristics were used for the analysis. The analytical results, which are summarized in Table 3 show excellent overall agreement with the NBS average and range values, even though the Fe content varied from >99 wt. % (NBS-19g) down to <1 wt. % (NBS 169). Thus, the use of a pure Fe solution as a blank for background corrections and as a matrix for preparing reference solutions for instrument calibrations is apparently valid.

TABLE 3. Accuracy data for Steel Analyses

Element	NBS		Wt %			NBS value, wt %	
	Sample No.	Matrix	System 1	System 2	System 3	Av	Range
Al	10g	Open hearth(0.2%C)	0.032	0.033	0.030	0.031	0.027-0.033
	33c	3 Ni	0.033	0.037	0.031	0.032	0.030-0.034
	169	77 Ni-20 Cr	0.095	0.10	0.130	0.095	0.095-0.105
Cr	19g	Open hearth(0.2%C)	0.37	0.37	0.36	0.374	0.369-0.380
	33c	3Ni	0.055	0.052	0.051	0.052	0.049-0.056
	129	Bessemer(0.1%C)	0.018	0.020	0.021	0.018	0.014-0.019
Cu	160	19 Cr-9 Ni-3 Mo	0.051	0.05	0.048	0.053	0.047-0.06
	169	77 Ni-20 Cr	0.014	0.014	0.015	0.015	0.013-0.02
	341	20 Ni-2 Cr	0.15	0.13	0.15	0.152	0.145-0.159
Mn	19g	Open hearth(0.2%C)	0.56	0.59	0.57	0.55	0.55-0.559
	33c	3Ni	0.73	0.73	0.78	0.73	0.73-0.735
	73c	Stainless steel	0.33	0.31	0.28	0.33	0.325-0.34
Ni	73c	Stainless steel					
		13 Cr	0.24	0.23	0.220	0.246	0.241-0.255
	111b	1 Mn-2 Ni	1.80	1.78	1.82	1.81	1.80-1.83

The background/stray light problem in trace analysis

When atomic emission spectroscopy is employed for the determination of trace elements at concentration levels near the detection limit, the spectral background is normally a large fraction of the total measured signal. For samples of varying composition, changes in the concentrations of concomitants often produce changes in background levels. These background shifts may be caused by true spectral line or band interferences, by changes in the spectral background continuum underlying the analysis lines, or by stray light contributions. If these background shifts occur, and appropriate corrections are not made, analytical biases may result. These biases may masquerade as interelement or a 'matrix' effects, when in reality the failure to recognize these spurious background effects is responsible.

Shifts in the true spectral background may arise from changes in the intensity of characteristic line or band emission from the concomitants. In many instances the relative intensity of these characteristic spectra from concomitants are so weak that they are not listed in even the most detailed wavelength tables. The unequivocal characterization of these background problems usually requires observations on the spectra of pure reference samples free of the analyte species. The general unavailability of such reference samples remains one of the unsolved problems of ultratrace analysis by atomic spectroscopy.

With reference to shifts in the real spectral continuum background caused by changes in the concentration of concomitants, natural line broadening effects may make substantial contributions. In a high temperature source, such as the inductively coupled plasma, the 'wings' of certain lines may contribute a significant continuum at wavelengths as far removed as 10 nm or more. For example, wavelength profile observations made with an ICP/double monochromator facility on the Ca lines at 393.4 and 396.8 nm reveal that the natural line broadening effect from the presence of 100 µg/ml of Ca in the nebulized solution produces a signal equivalent to ≈0.03 µg/ml of Al at the Al 396.2 nm line. In the selection of analyte lines, proper consideration should therefore be given to line broadening contributions. Because the alkaline earth elements are highly ionized in the plasma, their ion resonance emission lines are unusually intense. For example, at 1000 µg/ml Ca, the lines at 393.4 and 396.8 possess line/background ratios of ≈1 x 10⁶. Special care must therefore be exercised in selecting analysis lines in the proximity of the ion lines of the alkaline earth elements, especially if the latter undergo significant variations in concentration from sample to sample.

Larson et al. (34) have recently identified the various sources of stray light arising from defects in the optical components, design, and engineering of optical spectrometers. Undoubtedly stray light effects have often occurred in the past but have not been recognized because analyses were not performed near detection limit concentrations, or the effects of stray light were obscured by indirect effects on the real spectral background, or other interelement interactions caused far greater excursions in net line intensities. Because of the unusually low degree of interelement interactions in the atomization-

excitation process in ICP's, changes in the stray light are not as readily obscured by other effects and are thus more readily discernible.

General stray light levels may be decreased significantly through the use of "state of the art" gratings and optical components as well as through quality engineering in the design of spectrometers. Thus, the judicious application of optically-flat, black coatings to all potential non-optic reflecting surfaces, the installation of optical baffles or tunnels to trap zero and other order radiations and to prevent "cross talk" between optical channels, and the blockage of exit slits that isolate very intense lines, have reduced the overall general stray light level of the polychromators in our laboratory to tolerable proportions.

The reduction of the total stray light level to insignificant proportions for all sample types is not possible, because a fraction of this radiation arises from imperfections in the grating itself. Progressive improvements in grating production and replication in recent years have significantly reduced stray light originating from grating imperfections. For instance, the intensity of first order Rowland ghosts have been reduced from as great as 2% of the parent line for gratings ruled under mechanical control to <0.001% for gratings ruled under interferometric control. Some of the early gratings ruled under interferometric control exhibited high levels of far scatter ($\Delta\lambda > 5\text{nm}$) arising from imperfections in each grating ruling. These imperfections generally were caused by jitter in the ruling diamond as the servo-control system sought the null-position. Refinements in the control systems have resulted in significant reduction in far scatter. Holographically recorded gratings, which are recordings of an interference phenomenon, do not exhibit line ghosts and, through the use of virtually grainless photopolymers, also exhibit low levels of far scatter. Although the far scatter level of these gratings is low, it may still contribute a significant background signal at wavelengths far removed from the parent lines. For example, at 1000 $\mu\text{g/ml}$ of Ca, the scatter of intense Ca lines at 393.4 and 396.8 nm by the grating and other surfaces contributes a signal at the Zn 213.9 nm line equivalent to 0.02 $\mu\text{g/ml}$ of Zn, an intolerable level for determinations of this element at the ultratrace level. Thus for some ultratrace determinations, especially in samples containing variable concentrations of alkaline earth elements, the scatter stray light should either be removed optically or appropriate background corrections should be applied. Preliminary results have revealed that empirical correction coefficients based on a linear relationship with the interferent element concentration do not generally provide valid corrections. These results imply that either correction curves should be established or the coefficients should be based on measured intensities of the parent line or lines. The task of data collection and computation associated with these corrections is greatly simplified when polychromators are employed, because the parent concomitant intensities from which correction coefficients are calculated can be measured simultaneously. Stray light arising from the cumulative effect of many elements or lines may necessarily complicate the correction procedure.

In many cases sufficient rejection of far scatter radiation may be achieved with narrow bandpass interference filters placed immediately in front of the detectors in a polychromator or in front of the entrance slit of a monochromator, if determinations are made sequentially. This approach has been evaluated for a variety of ultratrace analytical problems, such as the determination of part per billion levels of cationic pollutants in hard and soft waters, in foods of variable ash composition and in urine. These evaluations have shown that the far scatter intensity in the 190 to 230 nm region arising from the Ca 393.4 and 396.9 nm lines, when the Ca concentration levels are as high as 1000 $\mu\text{g/ml}$, is reduced to negligible proportions for most applications. The same degree of success has not been achieved with similar experiments involving the intense Mg 279.6 and 280.2 nm parent lines. These observations suggest that changes in the Mg concentration from zero up to 1000 $\mu\text{g/ml}$ causes an increase in the real spectral background in the 190 to 230 nm region. Double monochromators that provide very high stray light rejection factors have been found to eliminate the need for stray light corrections for many ultratrace applications.

Analytical Applications

A recent review by Greenfield et al. (9) cites many of the analytical applications of ICP-AES systems published at the time the review was prepared. The materials analyzed ranged from metals and alloys, minerals and refractory oxides, whole blood and serum, oils and organic compounds, soils, effluents, mineral acids, and rare earth. Recent published applications include The determination of U in rocks (35), wear metals in lubricating oil (36), alloying and impurity elements in low and high alloy steels (37), sputtered material from thin films (38), rare earth mixtures (39), geochemical samples (40), and plant materials (41).

REFERENCES

1. A. Walsh, Spectrochim. Acta, **7**, 108-117 (1955).
2. T. B. Reed, J. Appl. Phys., **32**, 821-824, 2534-2535 (1961).
3. T. B. Reed, Intl. Sci. Techn., 41-48 June, 1962,
4. H. U. Eckert, High Temp. Sci., **6**, 99-134 (1974).
5. S. Greenfield, I. L. Jones, and C. T. Berry, Analyst, **89**, 713-720 (1964).
6. R.H. Wendt and V. A. Fassel, Anal. Chem., **37**, 920-922 (1965).
7. V. A. Fassel, Plenary Lectures-Colloquium Spectroscopicum Internationale XVI, pp. 63-91, Adam Hilger, Ltd., London (1972).
8. V. A. Fassel and R. N. Kniseley, Anal. Chem., **46**, 1110A-1120A, 1155A-1164A (1974).
9. S. Greenfield, H. McD. McGeachin, and P. B. Smith, Talanta, 1-14 (1976).
10. S. Greenfield, Proc. Soc. Anal. Chem., **2**, 111-113 (1965).
11. G. W. Dickinson and V. A. Fassel, Anal. Chem., **41**, 1021-1024 (1969).
12. V. A. Fassel, Hasler Award Address, Tenth National Meeting Society for Applied Spectroscopy, St. Louis, Oct. 20, 1971; Paper #83, Eleventh National Meeting, Society for Applied Spectroscopy, Dallas, Texas, Sept. 14, 1972.
13. P.W.J.M. Boumans and F. J. de Boer, Spectrochim. Acta., **30B**, 309-334 (1975).
14. K. W. Olson, W. J. Haas, and V. A. Fassel, Anal. Chem., in press (1976); presented at Federation of Analytical Chemistry and Spectroscopic Societies Meeting, Philadelphia, Pennsylvania, November 15, 1976.
15. R. H. Scott, V. A. Fassel, R. N. Kniseley, and D. E. Nixon, Anal. Chem., **46**, 75-80 (1974).
16. D. J. Kalnicky, R. N. Kniseley, and V. A. Fassel, Spectrochim. Acta, **30B**, 511 (1975).
17. R. H. Wendt and V. A. Fassel, Anal. Chem., **38**, 337-338 (1966).
18. V. A. Fassel and G. W. Dickinson, Anal. Chem., **40**, 247-248 (1968).
19. R. N. Kniseley, A. Amenson, C. C. Butler, and V. A. Fassel, Appl. Spectrosc., **28**, 285-286 (1974).
20. J. L. Jones, R. L. Dahlquist, and R. E. Hoyt, Appl. Spectrosc., **25**, 628-635 (1971).
21. R. L. Dahlquist, J. W. Knoll, and R. E. Hoyt, Application of the Inductively Coupled Plasma Using Thermal and Direct Aerosol Generation, Applied Research Laboratories Report, Sunland, California (1974).
22. H. C. Hoare and R. A. Mostyn, Anal. Chem., **39**, 1153-1155 (1967).
23. G. W. Dickinson, Application of the Induction Coupled Plasma to Analytical Spectroscopy, Ph.D. Thesis, Iowa State University, Ames, Iowa (1969).
24. R. M. Dagnall, D. J. Smith, T. S. West, and S. Greenfield, Anal. Chim. Acta, **54**, 397-406 (1971).
25. J. D. Chase, J. Appl. Phys., **40**, 318-325 (1969); **42**, 4870-4879 (1971).
26. S. Greenfield, I. L. Jones, H. McD. McGeachin, and P. B. Smith, Anal. Chim. Acta, **74**, 225-245 (1975).
27. J. C. Souilliant and R. P. Robin, Analisis, **1**, 427-433 (1972).
28. P.W.J.M. Boumans and F. J. de Boer, Spectrochim. Acta, **27B**, 391-414 (1972).
29. G. F. Larson, V. A. Fassel, R. H. Scott, and R. N. Kniseley, Anal. Chem., **47**, 238-243 (1975).
30. R. Herrmann, C. Th. J. Alkemade, and P. T. Gilbert, Chemical Analysis by Flame Photometry Interscience, N. Y. (1963).
31. V. A. Fassel and D. A. Becker, Anal. Chem., **41**, 1522 (1969).
32. A. C. West, V. A. Fassel, and R. N. Kniseley, Anal. Chem., **45**, 1586-1593 (1973).
33. C. C. Butler, R. N. Kniseley, and V. A. Fassel, Anal. Chem., **47**, 825-829 (1975).
34. G. F. Larson, V. A. Fassel, R. K. Winge, and R. N. Kniseley, Appl. Spectrosc., in press.
35. R. H. Scott, A. Strasheim, and M. L. Kokot, Anal. Chim. Acta, **82**, 67-77 (1976).
36. V. A. Fassel, C. A. Peterson, F. N. Abercrombie, and R. N. Kniseley, Anal. Chem., **48**, 516-519 (1976).
37. C. C. Butler, R. N. Kniseley, and V. A. Fassel, Anal. Chem., **47**, 825-829 (1975).
38. G. E. Thomas, E. E. de Kluizenaar, L. W. J. van Kollenburg, and L. C. Bastings, Anal. Chem., **47**, 2357-60 (1975).
39. V. A. Fassel, R. N. Kniseley, and C. C. Butler, Analysis and Applications of Rare Earth Materials, O. B. Michelsen, Ed., pp. 71-86. Universitetsforlaget, Oslo (1973).
40. R. H. Scott and M. L. Kokot, Anal. Chim. Acta, **75**, 257-270 (1975).
41. R. H. Scott and A. Strasheim, Anal. Chim. Acta, **76**, 71-78 (1976).